CHALMERS
UNIVERSITY OF TECHNOLOGY

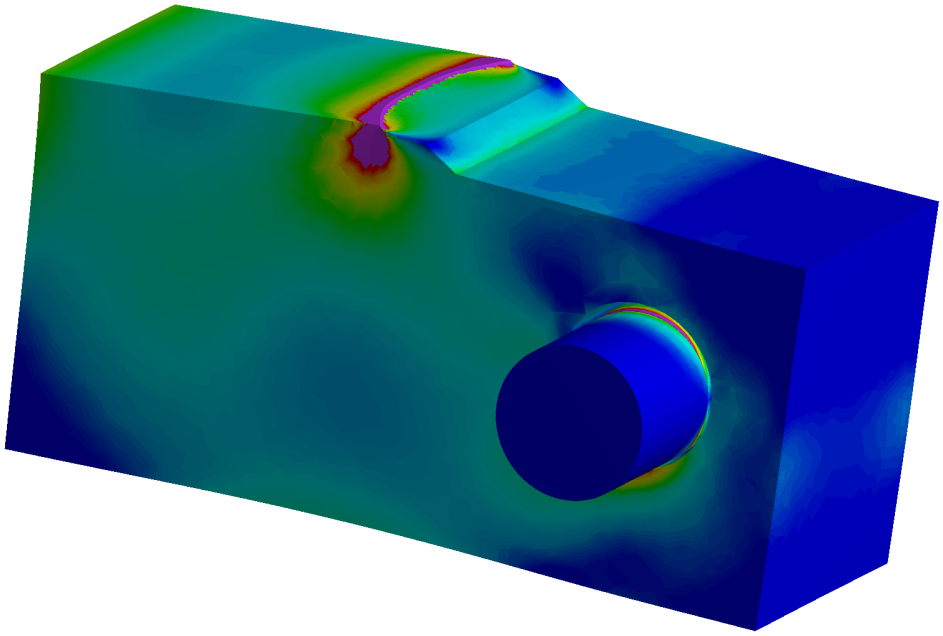

3-D Modelling of Plane-Strain Fracture Toughness Tests Using Ansys Workbench

Master Thesis at Chalmers University of Technology

Filip Wester Eric Gunnarsson

Department of Mechanics and Maritime Sciences
CHALMERS UNIVERSITY OF TECHNOLOGY
Gothenburg, Sweden 2020

Master Thesis MMSX30 2020

Report number 2020:38

3-D Modelling of Plane-Strain Fracture Toughness Test Using Ansys Workbench

CHALMERS
UNIVERSITY OF TECHNOLOGY

Department of Mechanics and Maritime Sciences
MMSX30
Chalmers University of Technology
Gothenburg, Sweden 2020

3-D Modelling of Plane-Strain Fracture Toughness Tests Using Ansys Workbench

Supervisor: Mats Delin and Tomas Månsson
Examinor: Anders Ekberg

Master Thesis 2020
Department of Mechanics and Maritime Sciences
MMSX30
Chalmers University of Technology

Typsnitt in LaTeX
Gothenburg, Sweden 2020

Abstract

This thesis shows the possibilities of modeling and recreating the fracture toughness test E399 using available test data. It also adds to the conclusion that for a excessive amount of plasticity the 95% secant can not be used to derive K_{IC} as the crack has not propagated at that point. Further it has been shown that for limited amount of plasticity the J-integral can be used to calculate the linear elastic stress intensity factor. The thesis also discusses the validity of adding friction between the specimen and the pin to increase the stiffness in the simulation to match the test data and compare this approach to other methods. Finally, ways of using FE modelling to get information from invalid tests are discussed.

Preface

The work presented in this thesis has been carried out at the Division of Dynamics within the department of Mechanics and Maritime Sciences at Chalmers University of Technology and at GKN Aerospace Engine Systems in Trollhättan. Professor Anders Ekberg have been the supervisor and examiner from Chalmers and with Mats Delin and Tomas Månsson as the supervisors at GKN Aerospace Engine Systems. We would like to thank Mats Delin, Tomas Månsson and professor Anders Ekberg for all their help, guidance and encouragement throughout this project. We would also like to thank Sushovan Roychowdhury and Peter Georgsson at GKN Aerospce Engine Systems for their valuable input and guidance to this thesis.

Contents

Nomenclature

a - Crack length
ANSYS - Computer program for FE-analyses
ASTM - American Society for Testing and Materials
CMOD - Crack mouth opening displacement
$\mathbf{d}A$ - Area of the propagated crack
$\mathbf{d}E$ - Change in total energy
$\mathbf{d}w$ - Work that is released as the crack propagates
$\mathbf{d}\Pi$ - Change in global potential energy
G - Energy release rate
GKN - Guest, Keen and Nettlefolds
K_I - Stress intensity factor for a Mode I crack
K_{IC} - Critical linear elastic stress intensity factor for Mode I crack
K_Q - Candidate critical linear elastic stress intensity factor
P_Q - Candidate critical force
J - Value of the J-integral
J_{el} - Elastic part of the J-integral
J_{IC} - Plain strain fracture toughness in terms of J
J_{pl} - Plastic part of the J-integral
K_J - Linear elastic stress intensity factor calculated using J-integral and non-linear elasticity under the assumption of J_{pl} being small
K_{JQ} - Linear elastic stress intensity factor calculated using J-integral and non-linear elasticity under the assumption of J_{pl} being small and obtained at the candidate critical force P_Q
$\mathbf{T}_i$ - Traction vector
W - width
CT - compact tension

1
Introduction

This thesis deals with analyzing fracture mechanics tests in particular K_{IC} testing using finite element simulations. The main objective was to see if a fracture toughness test could be replicated in FE analyses and what could be interpreted from the simulations.

When doing fracture toughness tests, sometimes the tests are invalidated meaning that one or more criteria stipulated in the testing procedure are violated. However, the tests can still be used, at least to get an estimate of fracture toughness values. This thesis aims at evaluating the fracture toughness tests broader by using numerical simulations.

This thesis shows that it may be possible to evaluate a stress-intensity factor using the J-integral at the critical candidate load even though the test is invalid. However it also shows that this value may not provide information about the fracture toughness as it is unsure if the crack has propagated at the indicated critical force.

1.1 Scope

1.1.1 Problem description

Throughout the years, different theories on fracture toughness testing have been put forward. Some being around plane strain toughness testing. Those theories have been assembled into ASTM E399. It has been found that there need to be some requirements on the testing procedure and responses in order to determine a material specific fracture toughness. If a test does not follow these requirements there is no way of retrieving a fracture toughness and the test can thus be seen as useless. However there is still some information from the test that can be useful. An example are the force to crack mouth opening displacement realtion, the proposed fracture toughness value K_Q and the specimen and pre-crack dimensions. This information makes it possible to model the test numerically and compare to the test.

1.1.2 Objectives

The main objective of this thesis is to develop a method for evaluating K_{IC} test results using FE-modeling based on linear elasticity and non-linear plasticity theories.

1.1.3 Limitations

No new tests will be carried out, only old test results will be used. Only CT tests will be used. Modelling of micro structures will not be carried out.

1.2 GKN Aerospace

The master thesis is produced at GKN Aerospace in Trollhättan Sweden. GKN was started in 1759 and stands for Guest, Keen and Nettlefolds. The airplane industry in Trollhättan started 90 years ago. The company is manufacturing and developing components for jet and rocket engines. They have jet components in more then 90 % of new larger airplanes around the world. The components are used in Airbus A320neo, A350, A380, Boeing 737MAX, 747, 787 and more. Also the jet engine RM12 for the Swedish military aircraft JAS 39 Gripen is produced, manufactured and maintained by GKN Aerospace.

2
Theory

2.1 Fracture mechanics

In the early years of fracture research there where concerns regarding infinite stresses at the crack tip. Since then studies have been made in order to find suitable ways to describe the stress conditions in a cracked structure.

2.1.1 Modes in loading

The crack face displacement can be expressed in three different modes shown in figure 2.1. Mode I is the opening mode loaded in tension. For Mode II the crack faces are sliding relative to each other in in-plane shear. Mode III is called the tearing mode or out-of-plane shear.

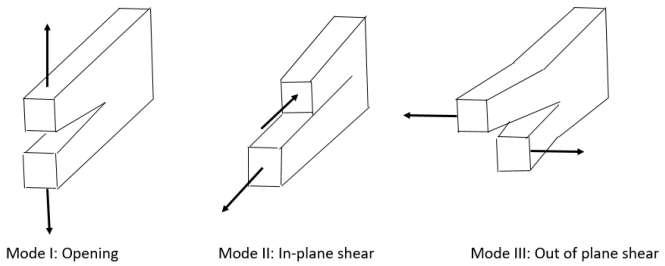

Figure 2.1: The three modes of loading.

2.1.2 Stress intensity factor K

The stress-intensity factor K is a parameter that quantifies the state of stress near the crack-tip in a linear elastic material. Equation 2.1 a to c, [1], describes the stress at the crack tip in mode I loading for the coordinate system shown in figure 2.2.

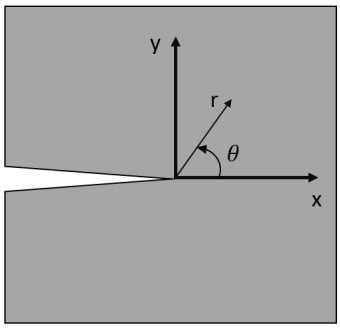

Figure 2.2: Coordinate system to calculate the stress.

$$\sigma_{xx} = \frac{K_I}{\sqrt{2\pi r}} cos\left(\frac{\theta}{2}\right)\left[1 - sin\left(\frac{\theta}{2}\right) sin\left(\frac{3\theta}{2}\right)\right] \tag{2.1a}$$

$$\sigma_{yy} = \frac{K_I}{\sqrt{2\pi r}} cos\left(\frac{\theta}{2}\right)\left[1 + sin\left(\frac{\theta}{2}\right) sin\left(\frac{3\theta}{2}\right)\right] \tag{2.1b}$$

$$\tau_{xy} = \frac{K_I}{\sqrt{2\pi r}} cos\left(\frac{\theta}{2}\right) sin\left(\frac{\theta}{2}\right) sin\left(\frac{3\theta}{2}\right) \tag{2.1c}$$

In plane stress

$$\sigma_{zz} = 0 \tag{2.1d}$$

If plane strain

$$\sigma_{zz} = \nu\left(\sigma_{xx} + \sigma_{yy}\right) \tag{2.1e}$$

Thus the general stress equation where θ is zero is described by equation 2.2.

$$\sigma = \frac{K_I}{\sqrt{2\pi r}} \tag{2.2}$$

K_I can be evaluated for different load cases based on how the load is applied and the geometry of the part. Specifics for the compact tension specimen case is explained in section 2.2.1.1.

2.1.3 K_{IC}

It has been found that materials fail at a critical magnitude of K, called the critical stress intensity or fracture toughness, K_{IC}. The fracture toughness of a material is dependent on temperature, corrosive environment, boundary effects etc. The fracture criterion can be stated as [2].

$$K_I \geq K_{IC} \tag{2.3}$$

K_I can be expressed analytically using equation 2.4.

$$K_I = f \cdot \sigma_\infty \sqrt{\pi a} \tag{2.4}$$

where f is a parameter that depends on load and geometry of the component and σ_∞ is the nominal stress.

As K is a description of the linear elastic stress intensity it is not applicable to fully describe the crack tip stress state at excessive yielding. In order to describe the crack tip state at excessive yielding the J-integral can be used see section 2.1.5.

2.1.4 Plastic zone

Due to the theoretical infinite elastic stresses at the crack tip there will be yielding which results in a plastic zone. Irwin estimated the plastic zone to have the size [3].

$$r_y = \frac{1}{2\pi}\left(\frac{K_I}{\sigma_{ys}}\right)^2 \tag{2.5}$$

As the stresses are redistributed when the zone starts yielding, a more accurate plastic zone estimation of the size is.

$$r_p = 2r_y = \frac{1}{\pi}\left(\frac{K_I}{\sigma_{ys}}\right)^2 \tag{2.6}$$

This redistribution effect is illustrated in figure 2.3.

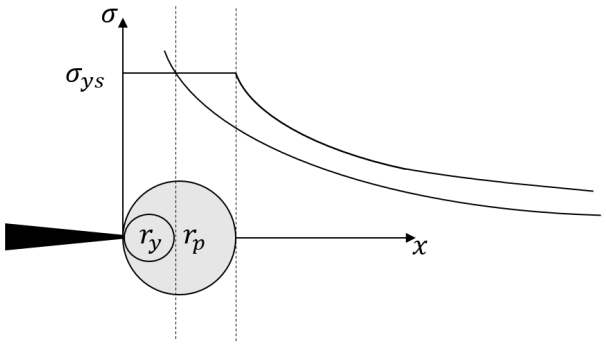

Figure 2.3: Crack tip plasticity. From [3]

Note that this is a simplification under plane-stress conditions. The plastic zone under plane-strain conditions is smaller.

Dowling [3] explains that LEFM is generally applicable if the crack size and the distance from the crack tip to a free edge is larger than $8r_y$ therefore a ligament size requirement can be explained by the following equation.

$$a, (w-a), h \geq 8r_y = \frac{8}{2\pi}\left(\frac{K_I}{\sigma_{ys}}\right)^2 = 1.27\left(\frac{K_I}{\sigma_{ys}}\right)^2 \tag{2.7}$$

Note the ASTM E399 also requires plane strain and therefore has a more stringent requirement explained in section 2.2.4.1.

2.1.5 J-integral

The J-integral can be defined as a line integral around the crack tip. The path independence of this line integral under certain conditions makes it possible to determine J for different crack lengths and geometries also for fairly large plastic deformations at the crack tip.

The path integral around a crack tip is given by the following expression [6].

$$J = \oint_{\Gamma} (w\, dy - T_i \frac{\partial u_i}{\partial x} ds) \tag{2.8}$$

Where Γ is an counter-clockwise arbitrary path around the crack tip, w is the strain energy density and is defined as $w = \int_0^{\epsilon_{ij}} \sigma_{ij} d\epsilon_{ij}$. T_i is the components of the traction vector on Γ and is evaluated as $T_i = \sigma_{ij} n_j$, where n_j is the component of the unit vector normal to the contour Γ. u_i is the displacement vector components, ds is a length increment along the contour Γ. X and y are the rectangular coordinates with y direction taken to the normal to the crack and the origin at the crack tip and can be seen in figure 2.4 below.

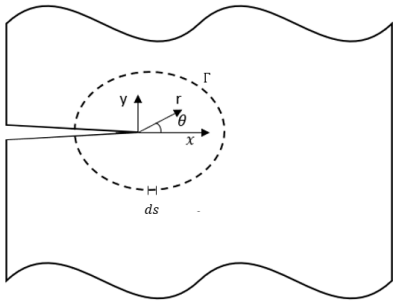

Figure 2.4: Crack tip used in the definition of J-integral.

The J value can be divided into an elastic and a plastic part as in equation (2.9) [1].

$$J = J_{el} + J_{pl} \tag{2.9}$$

The elastic part is:

$$J_{el} = \frac{K^2(1-\nu^2)}{E} \tag{2.10}$$

Where K is the stress intensity factor described in section 2.1.2. The plastic part can be expressed as.

$$J_{pl} = \frac{\eta A_{pl}}{B_N b_0} \tag{2.11}$$

A_{pl} is the area under the load-displacement curve shown in figure 2.5, b_0 is the ligament length. The dimensionless constant η is for a CT specimen, calculated as seen below from Anderson [1].

$$\eta = 2 + 0.522 \frac{b_0}{W} \tag{2.12}$$

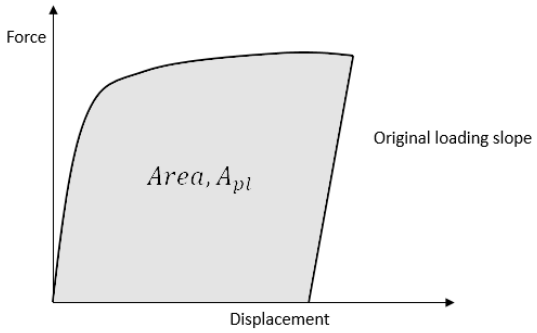

Figure 2.5: Plastic energy dissipated in the test specimen during crack growth test.

Thus if the plastic part is negligible ($J \approx J_{el}$) K can be calculated from rewriting equation 2.10 to.

$$K = \sqrt{\frac{JE}{(1-\nu^2)}} \tag{2.13}$$

In order to separate linear elastic stress intensity factor K the nonlinear stress intensity factor calculated from J using eq 2.13 will be noted as K_J.

2.2 Fracture toughness standard tests

The fracture toughness and critical stress intensity values are estimated from test results that are described in different standards. The one used for the tests in this thesis is the ASTM E399 [4]. It concerns loading of a fatigue pre-cracked specimen to final failure under linear elastic plane strain conditions. Under conditions of larger plasticity and/or smaller specimens ASTM E1820 [5] can be used. However this test is considerably more expensive.

2.2.1 ASTM E399 - Standard test method for linear elastic plane strain fracture toughness testing of metallic materials

The test method E399 is used to determine the fracture toughness K_{IC} under linear-elastic plane strain conditions. The method describes how the test should be carried out and which requirements that need to be fullfilled to get a valid K_{IC}.

2.2.2 Test procedure

The tests examined in this thesis where compact tension specimen, CT, see section 2.2.3. ASTM E399 also includes other specimen types. The CT specimen test is conducted by pulling the specimen open until it fails while measuring the force and crack mouth opening displacement, CMOD, see section 2.2.3 for a measurement description. To get an initial fatigue crack, the specimen is subjected to a pre-test cyclic loading until the crack is at a certain length. The fatigue crack is measured

after the test and added to the notch length to get the total crack length. The measured data is plotted with force as y and CMOD as x to get the force at which the specimen is starting to fail, the candidate load P_Q.

P_Q is seen in figure 2.6. The line O-P_5 is at a 95 % of the slope of O-A line which is the linear-elastic response. The O-P_5 is called the 95% secant. From the O-P_5 line P_Q is determined using the following three conditions: If the force P_Q is lower than P_5 (type I in figure 2.6), then $P_5 = P_Q$. If there instead is a maximum force that is larger then P_5 (type II and type III in figure 2.6) then the maximum force is taken as P_Q.

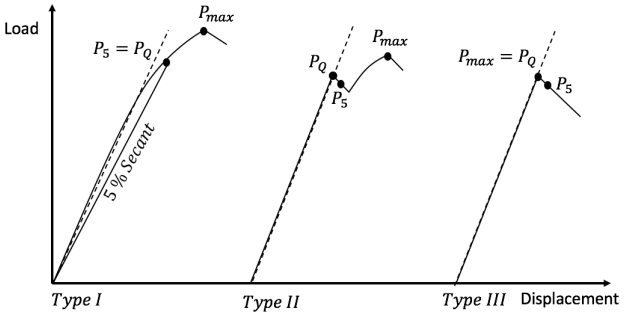

Figure 2.6: Force versus displacement (CMOD) for three different types.

2.2.3 CT specimen

The CT specimen is a side notch crack specimen subjected to pulling force in pin holes see figure 2.7.

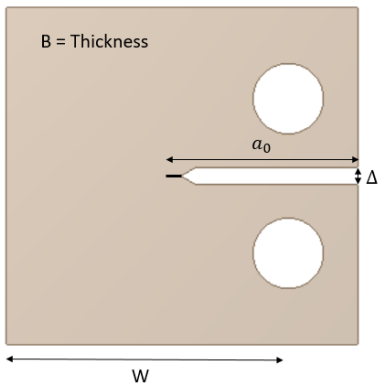

Figure 2.7: CT specimen with measures.

For a CT specimen the calculation of the candidate critical stress-intensity factor K_Q as stated in [4], is.

$$K_Q = \frac{P_Q}{\sqrt{BB_N}\sqrt{W}} \cdot f(\frac{a}{W}) \tag{2.14}$$

B is the thickness of the specimen, for plain sided specimens it should be measured close to the notch. B_N is the thickness between the roots of a side grooved specimen. The uncracked ligament size is W. The crack size is defined as a and is the distance from the crack front to the notch edge. If all requirements are satisfied then the critical stress-intensity K_{IC} can be determined as $K_{IC} = K_Q$.

2.2.4 ASTM E399 Requirements

There are requirements to assure a correct K_{IC} value from a test. These are all described in ASTM E399. Some of the requirements are regarding the procedure of the test and as none of these in the studied set of tests, broke these will not be described here. Other consider the length of the fatigue crack and the size of the cyclic load applied during the pre-fatigue cracking. Other requirements are to assure the correct geometry of the specimen. These are clearly explained in ASTM E399 and not broken in the studied tests so these will also not be explained further. The requirements broken in the examined tests where realted to excessive plasticity and P_{max}/P_Q ratio.

2.2.4.1 Excessive plasticity

The ligament size, $(W - a)$ as seen in figure 2.7, needs to satisfy the similarity $(W - a) > 2.5(\frac{K_{IC}}{\sigma_{ys}})^2$. This requirement will assure that the plasticity in the ligament is small enough to ensure a valid result. In order to describe the requirement, one can look at the plastic zone size where it is shown by equation 2.6 that, $8r_p = \frac{8}{\pi}\left(\frac{K_I}{\sigma_{ys}}\right)^2 = 2.5465\left(\frac{K_I}{\sigma_{ys}}\right)^2 \approx 2.5\left(\frac{K_I}{\sigma_{ys}}\right)^2$ Note that in section 2.1.4 Dowling [3] explains that the plastic zone for LEFM to be applicable is $8r_0$ not $8r_p$.
There are cross dimension requirements in ASTM E399 based on the ligament size requirement. These provide a restriction of the plastic zone in the thickness and crack-length. The cross dimensional requirements are: total crack length should be in the range of 0.45 and 0.55 times W. The thickness B is described as a ratio where W/B should be larger than 2 and less than 4. And the height is limited to $1.2 \cdot W$ not as a requirement but as a standard proportion [4].

2.2.4.2 P_{max}/P_Q ratio

Another important requirement is that P_{max} is not allowed to exceed $1.1 \cdot Pq$. According to Anderson [1] this is to ensure a correct K_{IC} value by neglecting materials with a steep resistance curve thus minimizing size effects on the K_{IC} value. Wallin [7] argues that this requirement also is to assure at least 2% crack growth before final fracture, which can be seen as equivalent to what Anderson is stating.

2.2.5 Test data

The information from the test report which was at hand was the following.

- Test temperature
- Specimen geometry, W, B, a, etc
- 5 measurements of the pre-fatigue crack
- Candidate load, P_Q
- Candidate stress-intensity, K_Q
- Force vs CMOD plot
- Plastic zone requirement validity and the underlying numbers
- P_{max}/P_Q ratio and the underlying numbers
- More requirements, mostly test procedure requirements
- Additional data that were not used

It was obvious that the validity for this material was heavily based on the temperature. The tests that were examined are presented in table 2.1. The only validated tests where those examined at 23.9 degrees.

Table 2.1: Test table.

Temp [C]	Test	$(W-a) > 2,5(\frac{K_Q}{\sigma_{YS}})^2$	$\frac{P_Q}{P_{max}}$
23.9	Test 1	Valid	Valid
23.9	Test 7	Valid	Valid
23.9	Test 31	Valid	Valid
150	Test 2	Invalid	Valid
150	Test 8	Invalid	Valid
150	Test 20	Invalid	Valid
150	Test 26	Invalid	Invalid
150	Test 32	Invalid	Invalid
250	Test 3	Invalid	Invalid
250	Test 9	Invalid	Invalid
350	Test 4	Invalid	Invalid
350	Test 10	Invalid	Invalid

2.2.6 Force-CMOD measurement

ASTM E399 is designed to retrieve K_{IC} which is calculated from the force P_Q. To receive the force, P_Q, the Force vs CMOD (crack mouth opening displacement) is measured. The CMOD, see figure 2.8, is measured using a self-supporting displacement clip gage. The gage is put on machined knife edges on the specimen mouth opening. There are certain requirements on these edges in E399, see Figure 2.9 which is a close up sketch of the clip gage mounting.

The force is measured using a loading rod. ASTM E399 requires the loading rod to be calibrated using ASTM E4, no more requirements are stated.

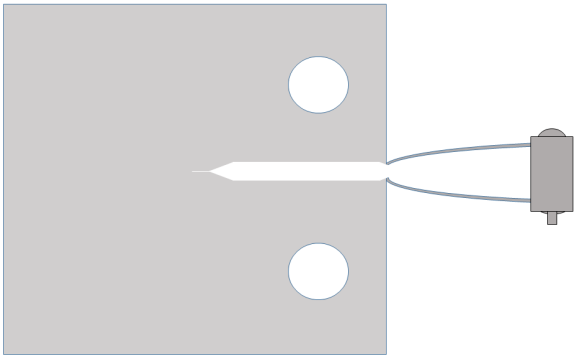

Figure 2.8: Sketch of the displacement gage [4]

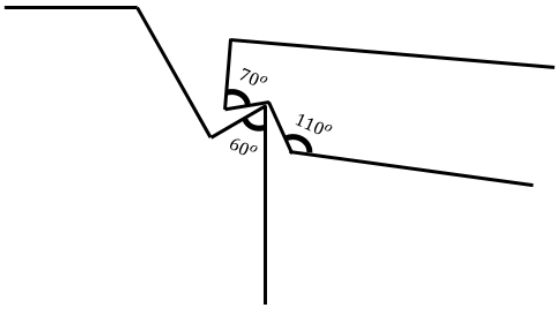

Figure 2.9: Close up on knife edges [4]

2.3 Literature review

Before and during the work with the thesis, literature was searched for to find approaches and answers to some of the issues involved.

The only work found that presented force vs CMOD curves comparison to test data was: *Linear and Non-Linear Stress Analysis for the Prediction of Fracture Toughness for Brittle and Ductile Material using ASTM E399 and ASTM E1290 by ANSYS Program package* [12]. This work indicated a lower stiffness from the simulation compared to the test data for the compact tension specimen. For the simulation a lower K_Q at critical load compared to test data was also shown.

Work was found where the ABAQUS FE program had been used. Unfortunately it did not present force vs CMOD comparison plots or evaluations of K. How the force was applied to the specimen in the simulations was also only described briefly [10].

Both of the above references modelled half specimens employing symmetry which indicated that such a model would be sufficient.

However, indications that friction would influence the test was found in [8] and [9].

3
Method

3.1 Modelling

The chosen approach was to model the system in Ansys and to verify the model by comparing it to the force versus CMOD curve. The K_Q value would be retrieved by loading the specimen to the measured force P_Q obtained from the test. This would be done both using linear (to get K_Q) and non-linear (to get K_{JQ}) analyses and by comparing the values to the analytical values from the test. It turned out that some of the Ansys simulations had too low stiffness as compared to test set-ups. The low stiffness was assumed to be caused by the presence of some friction in the test. This was assumed to be the best option as the material model and crack measurement errors would be to a small to cause the large differences found. A sensitivity analysis was made to check how much the measurement error would have to be to explain the discrepancy. This is discussed in chapter 5.

3.1.1 Model design

The geometry was sketched in design modeler based on the geometry specified in the test reports. To reduce simulation time, only half the specimen was constructed and a symmetry region was inserted in front of the crack. A pin was constructed in the loading hole in order to simulate the clevis pulling the specimen. The size of the pin was selected based on the ASTM standard. The pin was divided into three parts, one that were inside the hole and two that were outside of the hole. This made it easy to add boundary conditions.

The crack was constructed by splitting the face that divides the top and bottom of the specimen into two parts. One that represented the crack face and one that represented the symmetry region. The geometry of the fatigue precrack was obtained from the test reports where it was specified by 5 different measurements: Two at each side of the crack, two at the quarter points and one in the center of the crack, see figure 3.1.

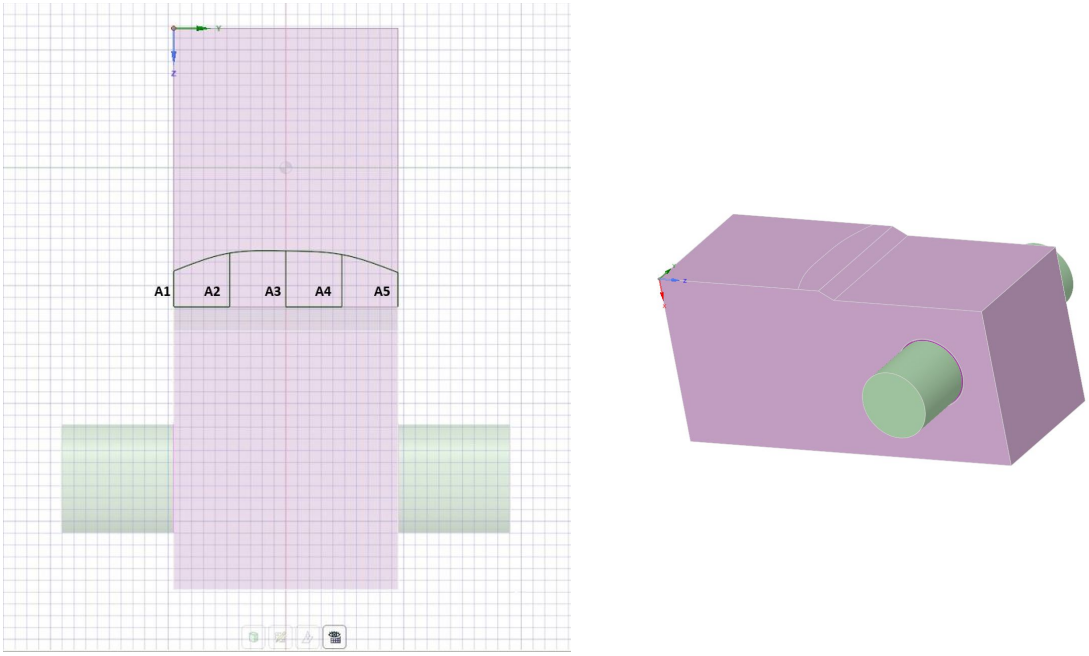

Figure 3.1: Sketch of the crack geometry.

3.1.2 Boundary conditions and finite element mesh

Once the 3D model was developed, the boundary conditions could be added to the parts. Displacement control was applied to the outer parts of the pin. A penalty contact condition was added between the inner part of the pin and the specimen. A friction coefficient was added to the pin-hole contact in order to adjust the FE model response to fit the Force-CMOD curve from the tests. This is further discussed in chapters 4 and 5. A symmetry boundary condition was imposed on the ligament ahead of the crack. The crack was specified as a pre-meshed crack with nodes positioned at the crack front line. The mesh was created with the mechanical auto generated mesh embedded in workbench with a resolution of 4 and an edge size on the crack-front. This was chosen based on the mesh study in section 3.2.

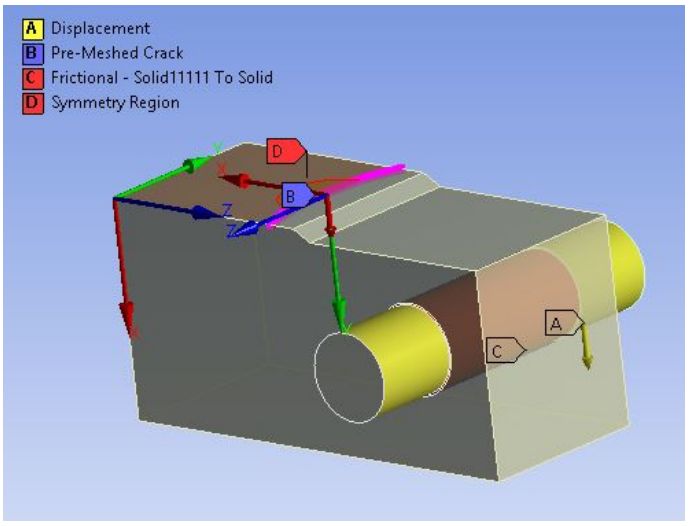

Figure 3.2: Boundary conditions of the specimen and the pin.

3.1.3 Comparison of numerical simulations and test results

From the Ansys simulation the force CMOD response was studied. The deformation probe calculates the displacement CMOD, crack mouth opening displacement. The force response is retrieved as the total force reaction on the displacement faces, see figure 3.3. These values where plotted against each other and compared to the experimental test data. The friction coefficient was increased or decreased iteratively until there was a good fit between the simulation and experimental test data.

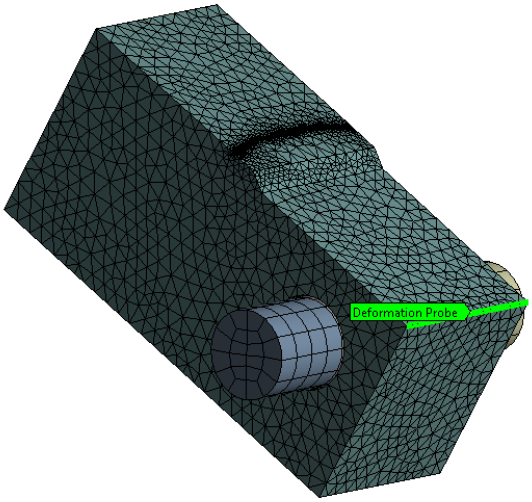

Figure 3.3: Deformation probe employed to calculate the CMOD

3.1.4 Stress intensity factors

To examine if there where low amounts of plasticity, the simulation was carried out both linear and non-linear by changing the material input in Ansys Workbench.

For the linear simulation the K value was extracted directly from Ansys. For the non-linear the K_Q-values where calculated by extracting the J-integral values and using equation 3.1.

$$K_{JQ} = \sqrt{\frac{E}{1-\nu^2}J} \tag{3.1}$$

The K values extracted using this approach were labeled K_{JQ} to diverse the values from those recived from the linear simulations.
Both the linear and non-linear candidate critical stress intensity factors where recived at the point where the pin reaction force was the measured P_Q from the test data.
To calculate the mean value of K_Q and K_{JQ} values from Ansys, the stress intensity and J-integral data were transfered in to Matlab. The negative values at the edge of the crack are removed. The stress intensity values were retrieved at a load magnitude related to the reaction force P_Q.

3.2 Validity and mesh convergence study

To evaluate the validity of the simplified model, two other levels of complexity were modelled. One with the full test without symmetry with the two clevises pulling. One without the clevises but still a full specimen with pins and also the simplified model described in section 3.1. The dimensions were based on the specifications in ASTM E399. The boundary conditions are shown in figures 3.4 to 3.8. The clevis displacement was put on the loading rod thread face, see figure 3.4, where also the reaction force was measured, see figure 3.5. The CMOD was measured on the tip of the specimen as shown in figure 3.3. For the model without the clevises the displacement was prescribed for the pins as shown in figure 3.6. The force was also measured on the displacement face. To test how the application of friction is dependent on the different models the connections were changed between frictionless and frictional with $\mu = 0.2$. Figure 3.9 and figure 3.10 shows how the connections where made for the model with the clevises.

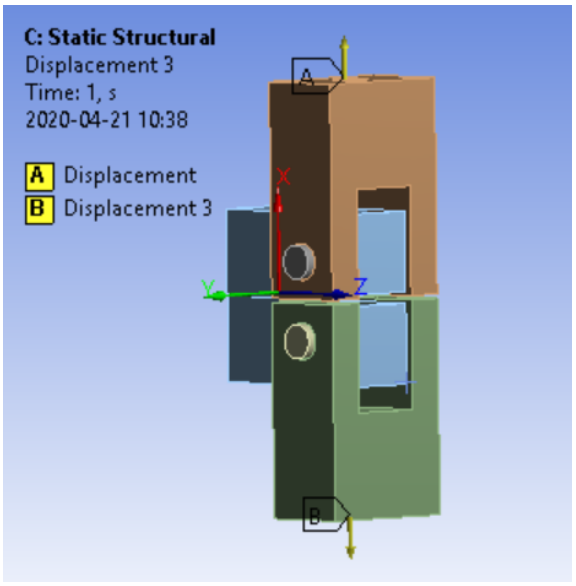

Figure 3.4: Model with clevis, displacement control.

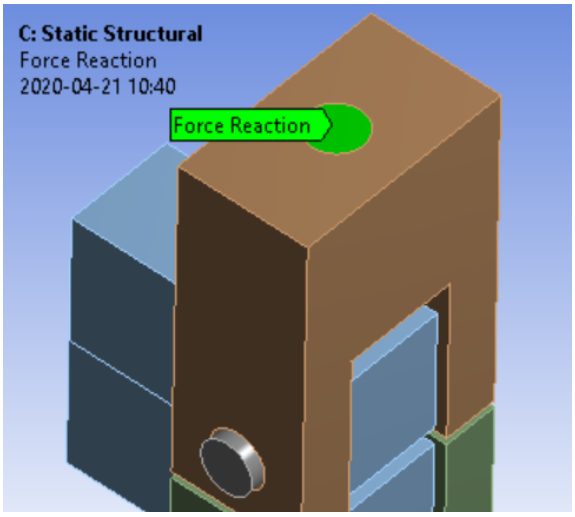

Figure 3.5: Model with clevis, force probe.

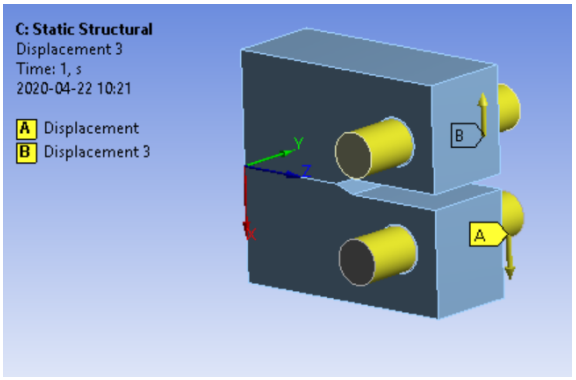

Figure 3.6: Model without clevis, displacement control.

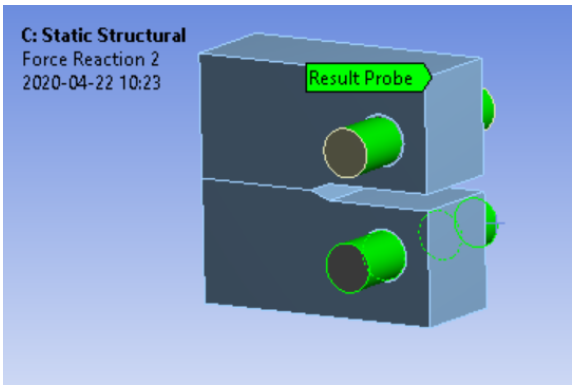

Figure 3.7: Model without clevis, force probe.

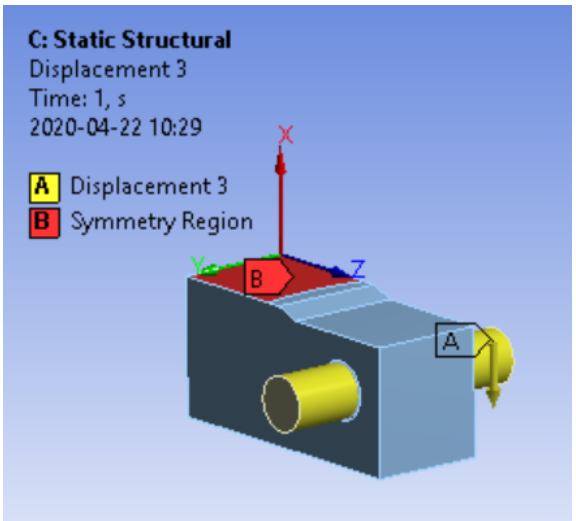

Figure 3.8: Model without clevis and with symmetry condition.

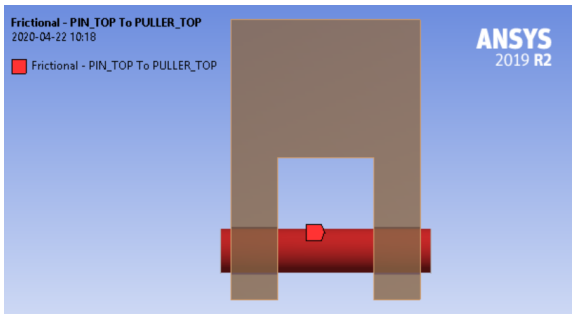

Figure 3.9: Contact clevis and pin.

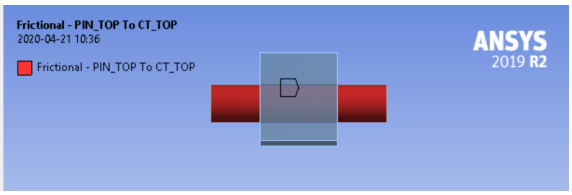

Figure 3.10: Contact specimen and pin.

The result from the comparison between simulations of different complexity levels are shown in figures 3.11, 3.12 and 3.13. Figure 3.11 shows force versus CMOD for frictionless contacts for moduls with and without clevis. The same comparition with friction in the pin and specimen interation is shown in figure 3.12. Figure 3.13 shows the result from only plotting the full model with the clevis while changing the friction coefficient. See section 3.1.4 for a description of the boundary conditions.

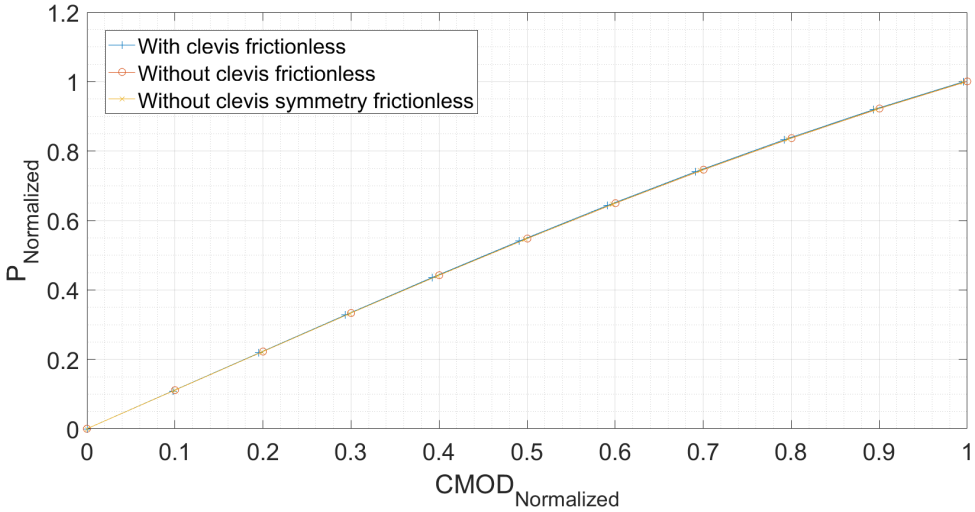

Figure 3.11: Comparison of simulation results featuring models with and without clevisfor frictionless contact.

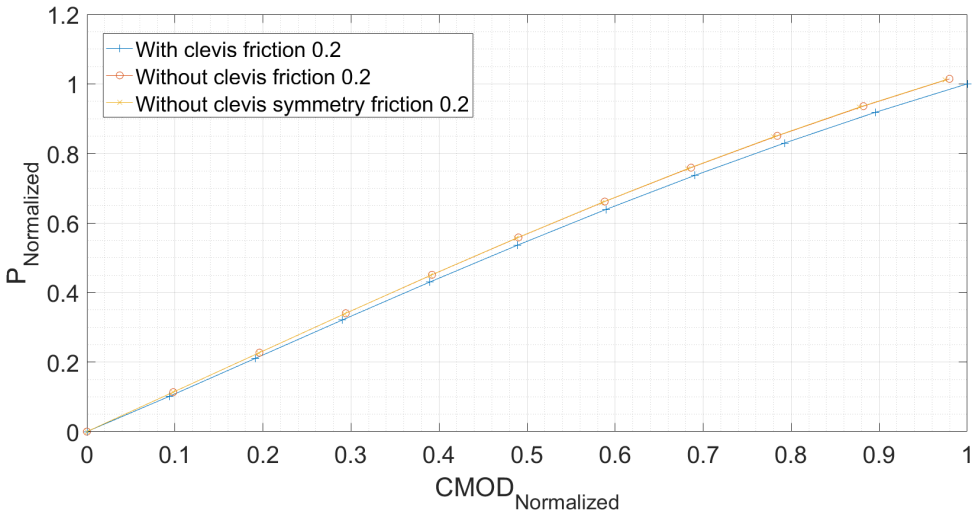

Figure 3.12: Comparison of simulations featuring models with and without clevis for frictional contact.

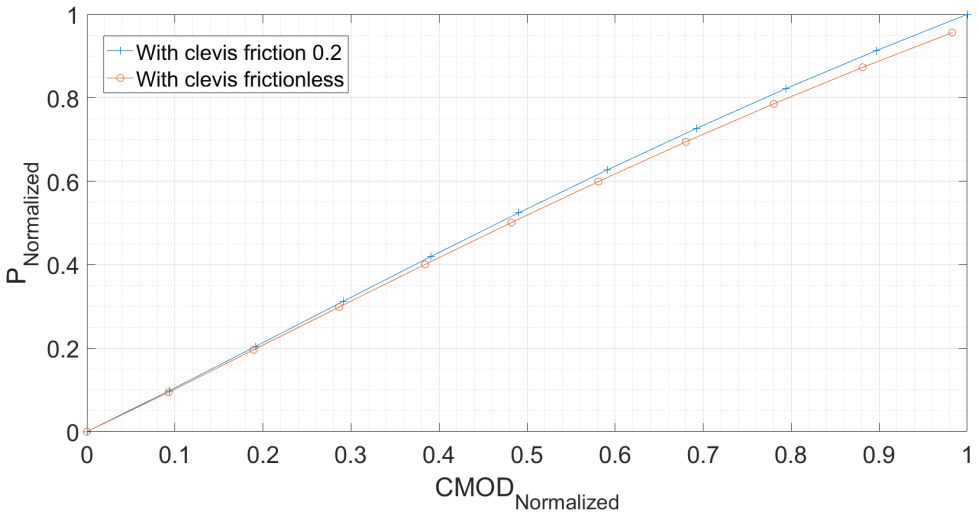

Figure 3.13: Comparison between frictional or frictionless contact results.

The conclusion from the complexity study was that the half specimen model was sufficient to get a good description of the force verus CMOD response. As the pin is not allowed to rotate in this set-up, the frictional constant is increasing compared to the full model with clevises, see figure 3.12. But figure 3.13 shows that the friction affects the stiffness in the full model with clevis but at a lower factor.

To determine which mesh density that is required, a mesh sensitivity study was made. The mesh was created using Ansys automatic meshing routine with a resolution and an edge size applied to the crack-front, see figure 3.15. The resolution was changed from 1 to 5 with the edge size reduced incrementally from 0.008 to 0.001. The value that would be most sensitive to mesh size at the crack front was

deemed to be the J-value. Therefor the mean J-value at the crack front was chosen as the comparison value. The second to last values, resolution 4 and edge size 0.002, where used as it was close to the last solution in figure 3.14. Note that this was the approach used in this case. If the edge size was decreased more rapidly then the resolution the mesh might have had a faster convergence.

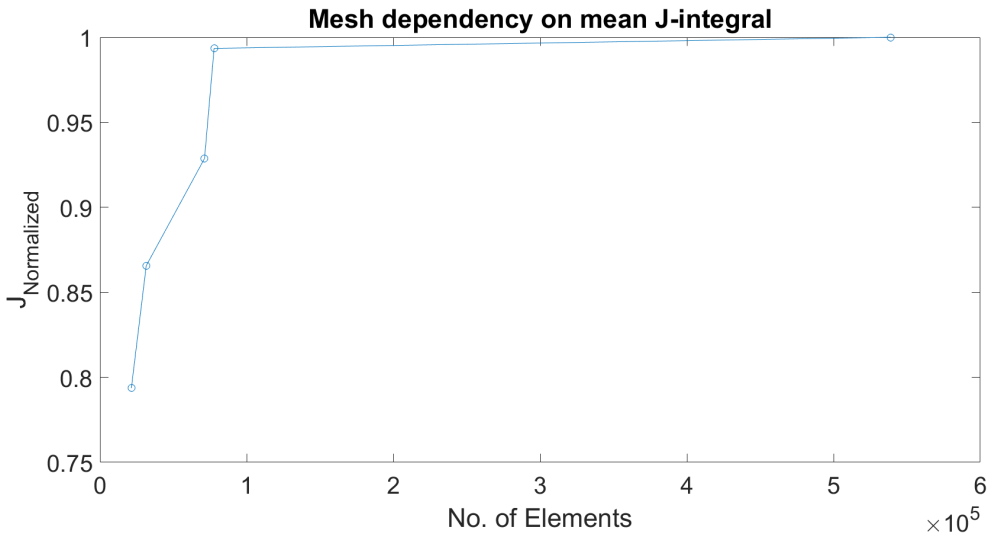

Figure 3.14: Mesh dependency study for mean J-integral.

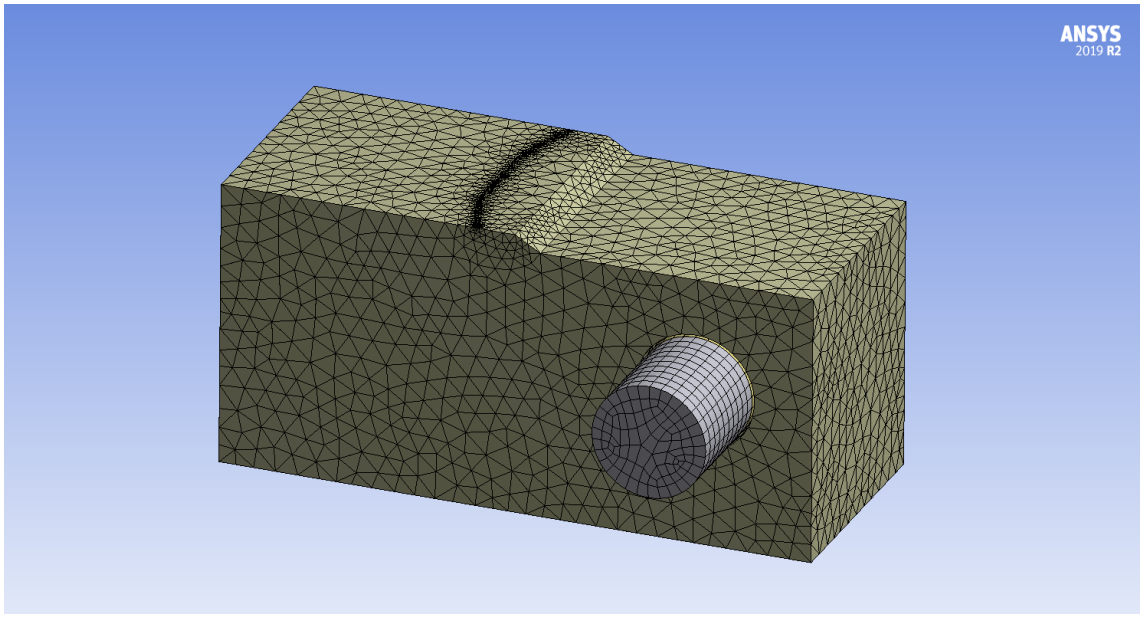

Figure 3.15: Final mesh

4

Results

4.1 Force versus CMOD comparisons between simulations and tests

In this section the results from the force vs CMOD comparisons are presented for different temperatures. The notation is that linear is employed for linear-elastic simulations, non-linear for elasto-plastic simulations. Table 4.1 contains information on whether the test is valid or not. In the table it is seen that most of the tests are invalid and that excessive plasticity is the hardest to avoid.
Results from the Ansys simulations showed that when friction was used, almost all simulations matched the force versus CMOD test data. The tests that were most difficult to match were tests 2 and 8 see figure 4.1 and 4.2. Common to these tests was that both had a large nonlinear zone in the initial loading. This discrepancy in force CMOD data also showed up when comparing K values from simulation and tests, see table 4.1 The difference is still small (5 % and 2 %) respectively and for non-linear simulations -2.8 and -2.6.

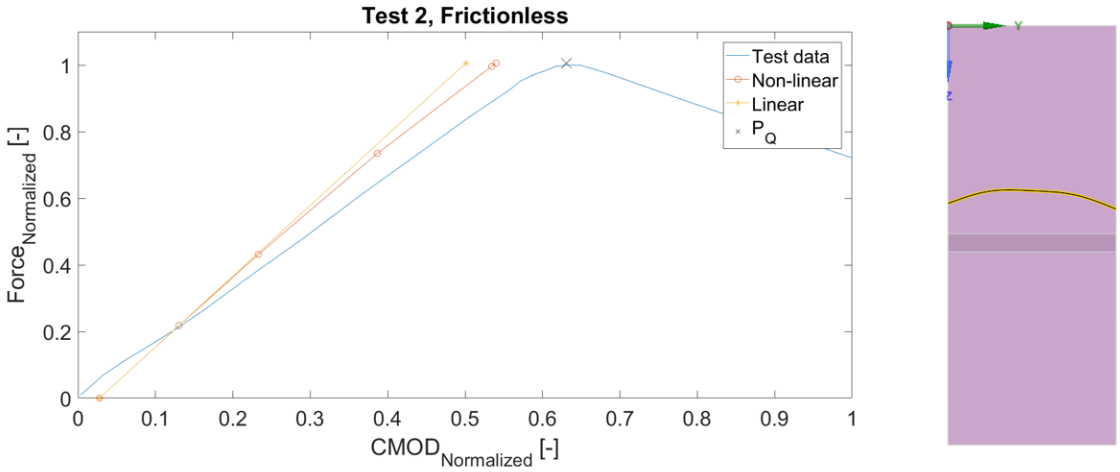

Figure 4.1: Force versus CMOD for test 2.

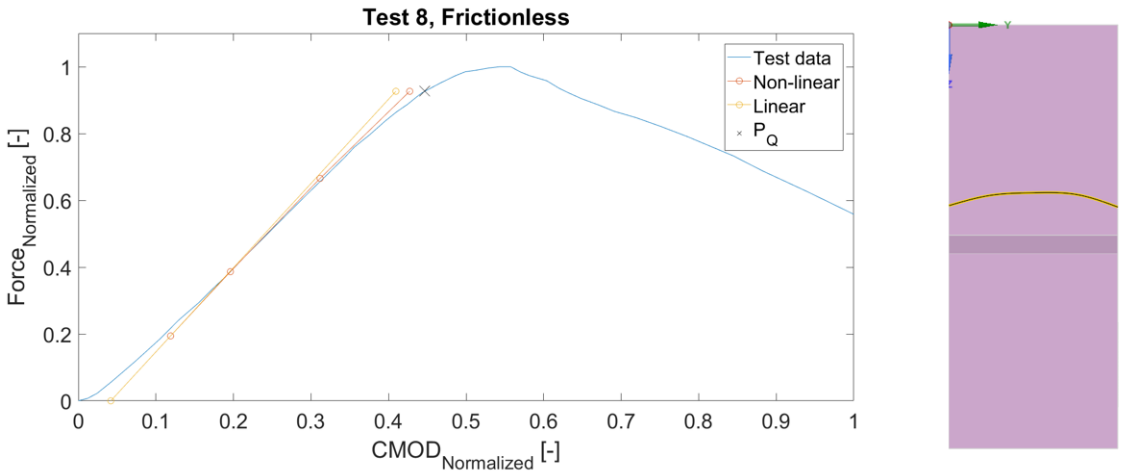

Figure 4.2: Force versus CMOD for test 8.

Looking at the tests that featured a good match to test data the response was heavily affected by the temperature and if they were invalid or not. Looking at the valid tests at 23.9 C, the linear and non-linear Ansys data were closely correlated, see for example figure 4.3, test 1. This indicated a low amount of plasticity and hence the tests were valid. The simulation also correlated to the test data up until P_Q where the compliance of the test started to increase indicating crack propagation.

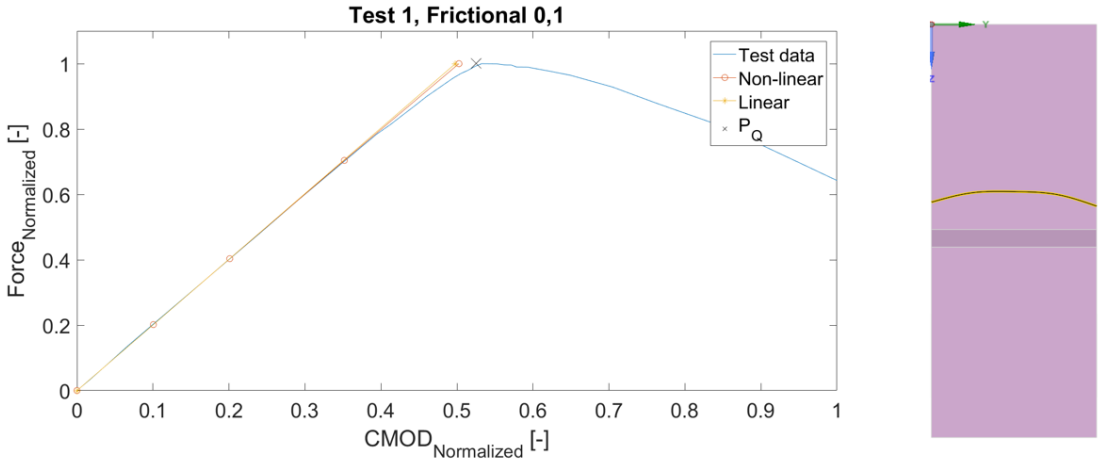

Figure 4.3: Force versus CMOD for test 1.

Test 20 was the only test that had a good correlation, was valid with respect to P_{max}/P_Q, but invalid with respect to plasticity, comparison between simulations and test data showed a tendency of higher compliance when the force is approaching P_Q, which indicates crack propagation see figure 4.4.

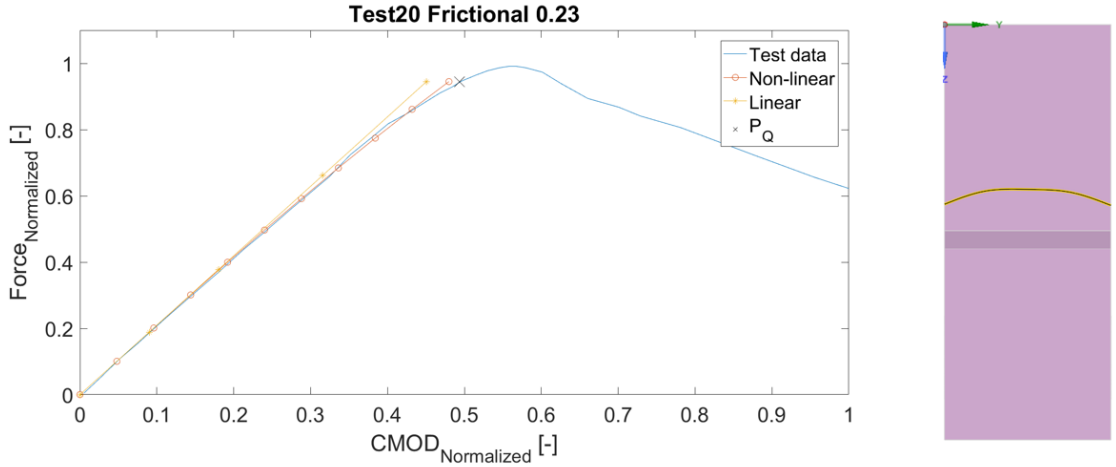

Figure 4.4: Force versus CMOD for test 20.

The remaining tests were all invalid with respect to both plasticity and resistance. This showed up in the force versus CMOD data as rather simular test responses. Test 3 is tested at 150 C and test 10 at 250 C both showing similar result. Looking at figures 4.5 and 4.6, the non-linear data follows the test data up until P_Q and beyond as shown in figure 4.7. This indicates that at the suggested P_Q from the 95% secant the crack has not propagated. This reinforces the suggestion from Wallin [7] that the stringent plasticity requirement in E399 is a consequence of securing crack growth using the 95% secant. The fact that the crack has not started to propagated also affects the P_{max}/P_Q requirement as it is not only affected by material resistance due to tearing but also by further plasticity until the crack starts propagating.

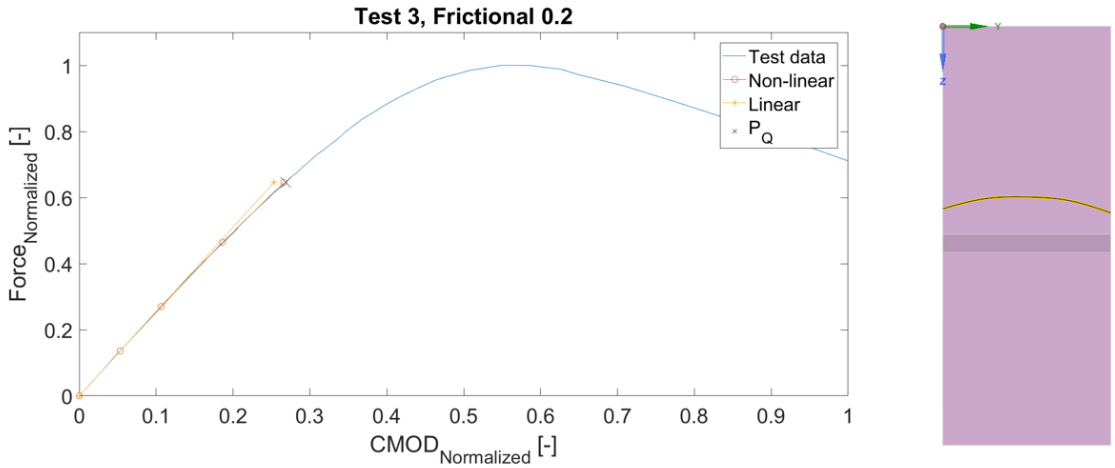

Figure 4.5: Force versus CMOD for test 3.

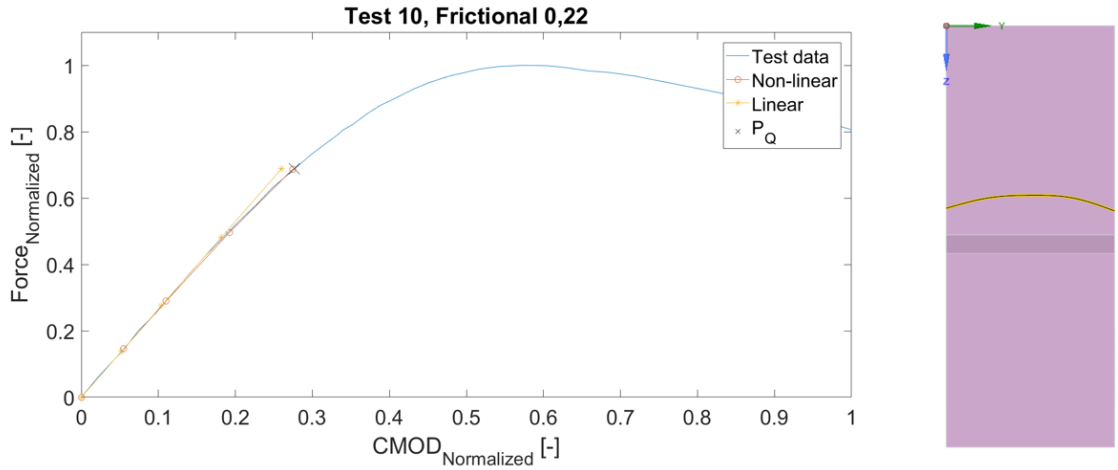

Figure 4.6: Force versus CMOD for test 10.

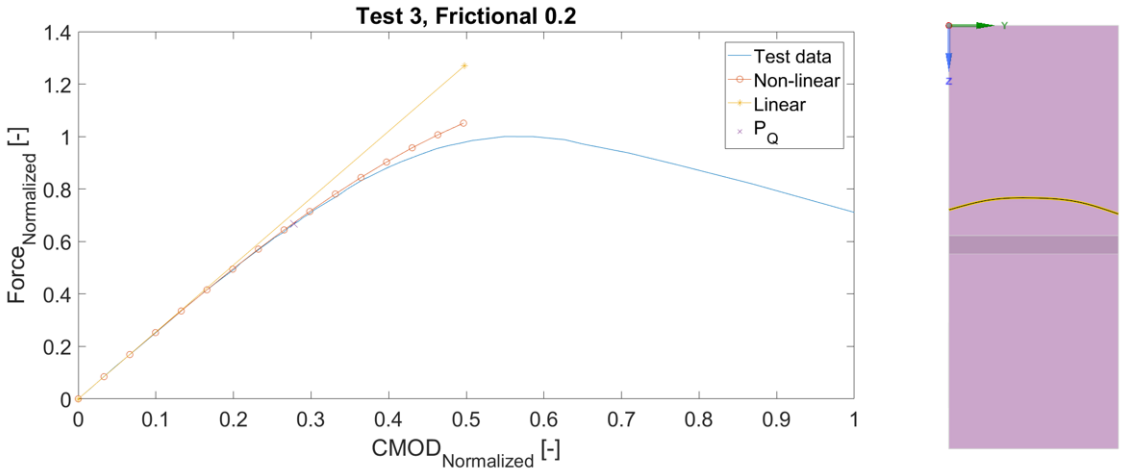

Figure 4.7: Force versus CMOD for test 3.

4.2 Stress intensities

To see if there is a varying stress intensity along the crack front and if it was affected by the validity of the , the numerically evaluated stress intensity was plotted along the crack front along with the stress intensity evaluated from the test. The stress intensity factor was evaluated at the instance of loading when the reaction force was P_Q. As with the force versus CMOD results, similar results were found for the different temperatures.

Test 1 (a valid test) is shown in figure 4.8. For this test, the linear, K_Q, and non-linear, K_{JQ}, stress intensities are closely correlated along the crack. Looking at the simulated stress intensity along the crack front in order to evaluate what the analytical value is representing, it is visible that the analytical stress intensity from the test is slightly higher than the numerically evaluated stress intensity in

a large region at the centre of the crack front indicating that the peaks in stress intensity magnitudes that arise at the specimen edges do have some influence on the analytical value. The averages from both of the simulations are also plotted. These are slightly lower than the mean which can be influenced by the big drop in stress intensity by the singularity at the absolute sides of the crack.

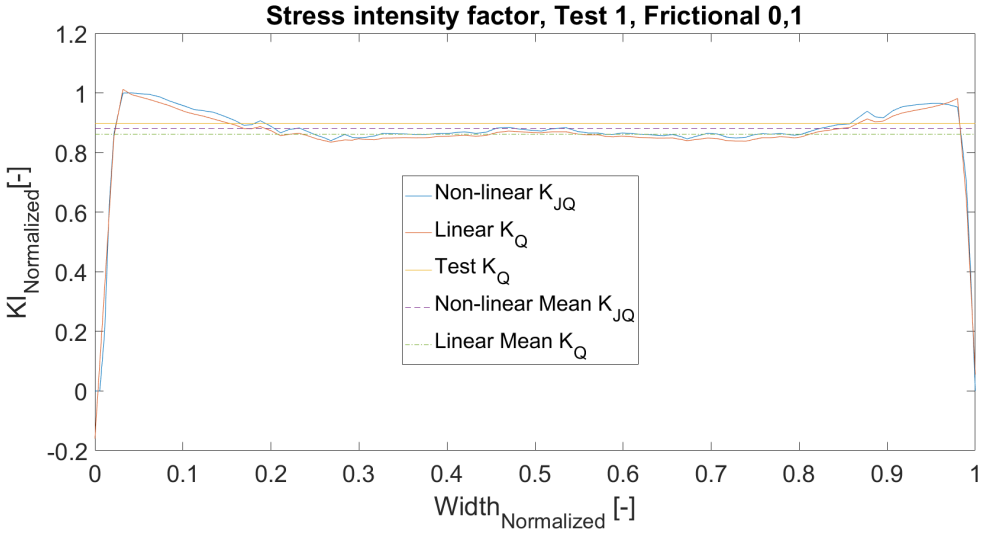

Figure 4.8: Stress intensity along crack front for test 1 at the load level P_Q.

The invalidated tests showed similar behaviour in force versus CMOD plots. One clear difference between the invalid tests and the valid tests is that K_{JQ} does differ more from K_Q values. The biggest difference is at the sides of the crack where the K_{JQ} does not seem to have as large peaks as K_Q. Also at the middle K_{JQ} exceeds K_Q, see test 10 (invalid), in figure 4.9. Test 10 is invalid in terms of both excessive plasticity and P_{max}/P_Q.

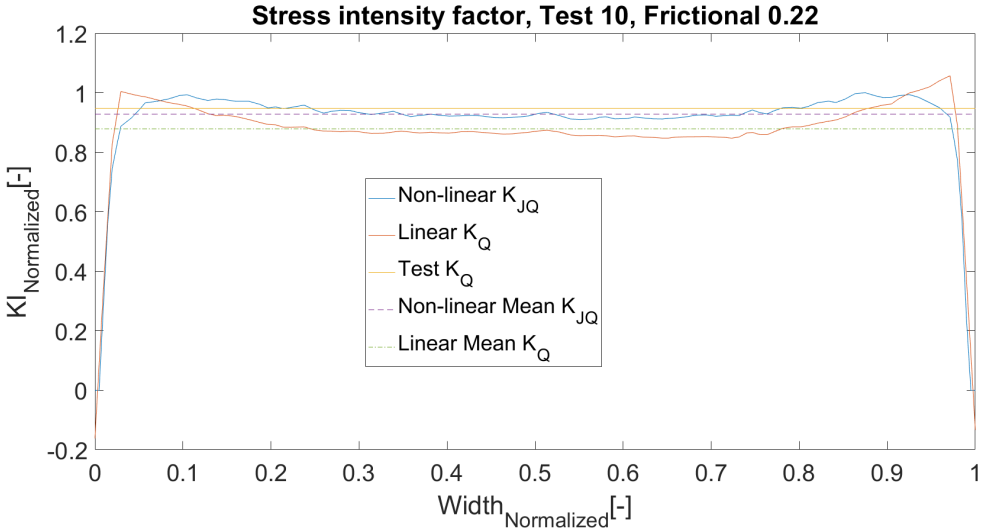

Figure 4.9: Stress intensity along crack front for test 10 at the load level P_Q.

In order to explain the response, the plastic zones for tests 1 and 10 were compared. In figure 4.10 it is seen that test 1 has a rather constant plastic zone size along the crack front, somewhat deeper at the sides. Test 10, figure 4.11, has a much larger zone at the sides which is likely to have caused the difference between K_Q and K_{JQ} along the crack.

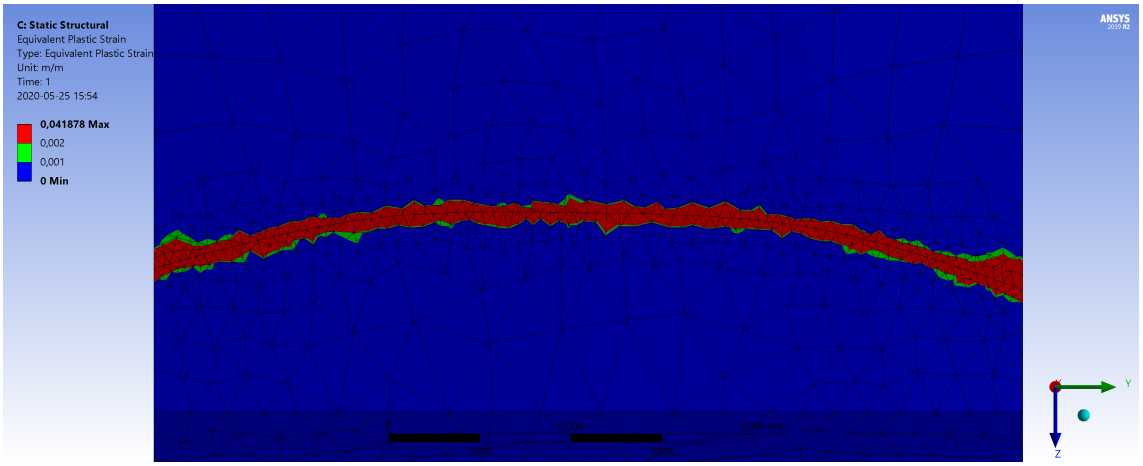

Figure 4.10: Plastic zone for Test 1.

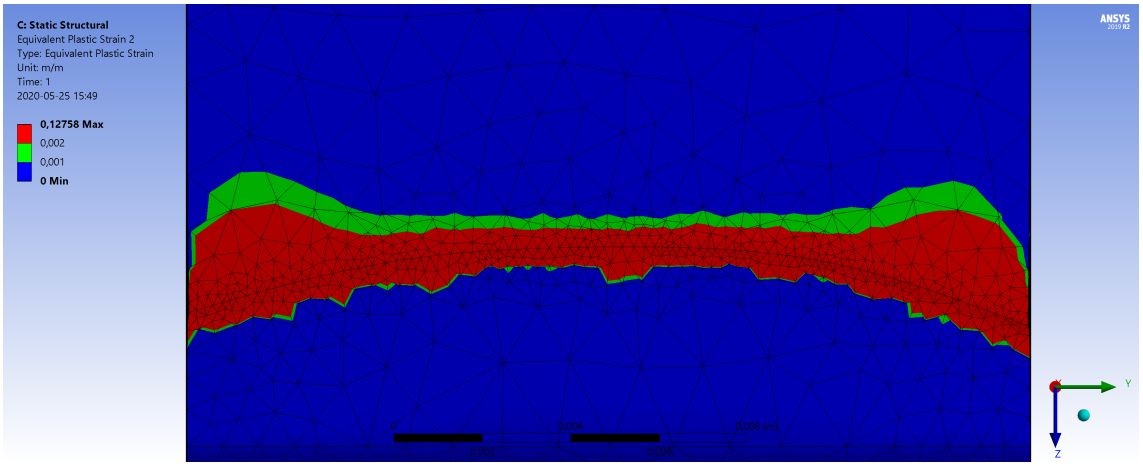

Figure 4.11: Plastic zone for Test 10.

4.3 Detailed test results

Table 4.1 presents the results from all examined tests. Column 1 shows at which temperature the test were carried out, column 2 shows the test number. Columns 3 and 4 in table 4.1 indicate the validity based on the different criteria stated in the column title. Columns 5 and 6 show the difference between test and simulations. % non-linear is the difference between the K_{JQ} mean value from Ansys and K_Q from the test. % linear is the percentage difference between K_Q mean value from Ansys and K_Q from the test.

Tests 1, 7 and 31 are valid in all aspects, but there is still a discrepancy between the test results and numerically evaluated K_Q. Tests 2 and 8 show, as expected from the force versus CMOD curves in figures 4.1 and 4.2, a clear difference in stress intensities as compared to the other test in the same temperature group.

The friction between pin and specimen seems to have some influence on the stress intensity value. Test 1, which has a substantially larger friction coefficient than tests 7 and 31, also has a larger difference between K_Q and K_{JQ}. The same trend is seen for test 32 in comparison to 20 and 26 and between tests 9 and 3 as compared to tests 10 and 4. The influence of friction coefficient on the stress intensity factor can be seen for both non-linear and linear materials.

Table 4.1: Results of tests.

Temp [C]	Test	$(W-a) > 2.5(\frac{K_Q}{\sigma_{YS}})^2$	$\frac{P_q}{P_{max}}$	Friction coeff	% Non-linear	% Linear
23.9	Test 1	Valid	Valid	0.1	-1.8	-4.0
23.9	Test 7	Valid	Valid	0	-0.6	-2.0
23.9	Test 31	Valid	Valid	0.01	-0.2	-2.3
150	Test 2	Invalid	Valid	0	4.8	-2.8
150	Test 8	Invalid	Valid	0	2.0	-2.6
150	Test 20	Invalid	Valid	0.2	-2.8	-8.5
150	Test 26	Invalid	Invalid	0.15	-2.0	-6.6
150	Test 32	Invalid	Invalid	0.08	-0.8	-5.3
250	Test 3	Invalid	Invalid	0.2	-1.3	-6.4
250	Test 9	Invalid	Invalid	0.1	-0.4	-9.3
350	Test 4	Invalid	Invalid	0.4	-2.9	-7.4
350	Test 10	Invalid	Invalid	0.22	-2.0	-7.3

5
Discussion and conclusion

5.1 Ansys modelling

The tests could be simulated in Ansys with good results. The tests that broke the excessive plasticity requirement reflected the test data more accurately than the valid tests indicating that the tests were yielding to such a degree that the 95% secant line could not describe the 2% crack propagation, [6].
A way to further describe the force CMOD response in Ansys is by investigating a propagating crack. To the author's knowledge this would have to be done using cohesive zone modelling as the smart crack growth functionality in Ansys only supports linear elastic material properties and it has been shown that the plasticity is affecting the response.

5.1.1 Influence of friction

The use of friction might not be the only reason for the increased stiffness in the tests. In the ASTM standard, the clevis should be flat on the bottom where the pin is touching the clevis. This has been shown to minimize friction effects between the clevis and the pin [8]. If a flat surface was used in the tests examined is not known but most likely. The magnitude of friction coefficient needed for the different tests is varying which could be caused by specimen differences or that there are some differences arising during the test. The reason for the friction to increase the force is described in figure 5.1, which show that the friction is resisting the specimen from turning. The same has been shown by Pook [9]. Pook shows that for a pin jointed single edge notch specimen the friction is reducing the turning moment by $M = \mu PW/6$ for a certain geometry. Where μ is the friction coefficient, P is the applied force and W is the uncracked ligament.

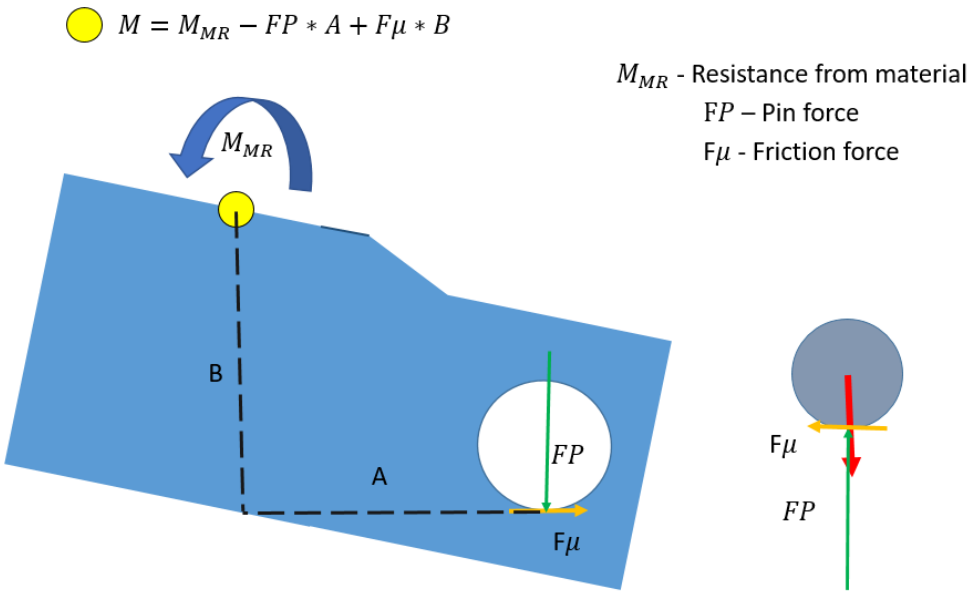

Figure 5.1: Moment equilibrium of the CT specimen

5.1.2 Alternative stiffness increasing properties

To check the validity of the hypothesis of the influence of friction, a simulation was conducted with one valid and one invalid test by changing different parameters to increase stiffness. Varied conditions were temperature, crack length, CMOD measurement and friction. The force versus CMOD results is presented in figure 5.2 and 5.3. It is seen that the change in parameters influence the stiffness and thus can because of seen as a liable reason for the discrepancy between the test and the simulations. As a comparison, results from a frictionless simulation with standard measurements is also plotted.

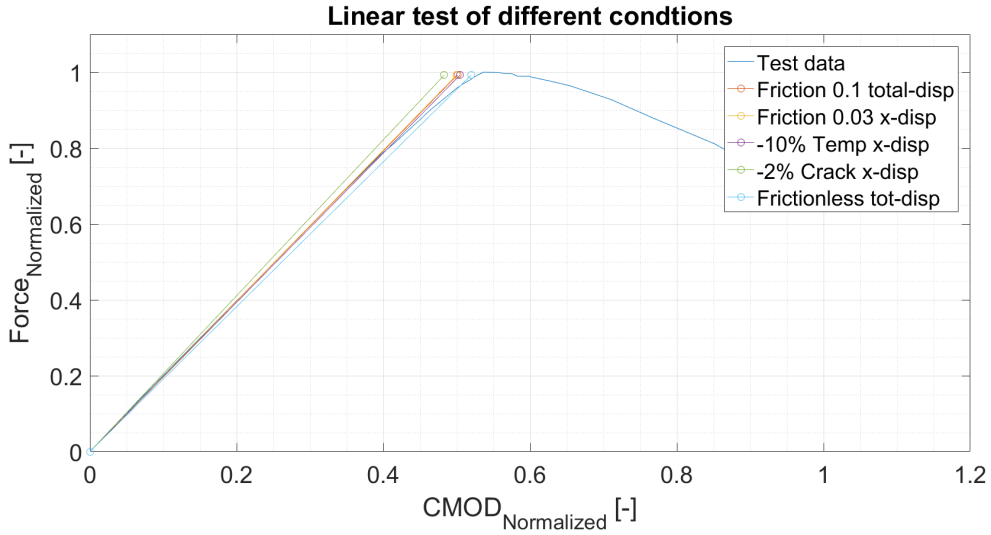

Figure 5.2: Prediction of force versus CMOD with linear material, under different conditions.

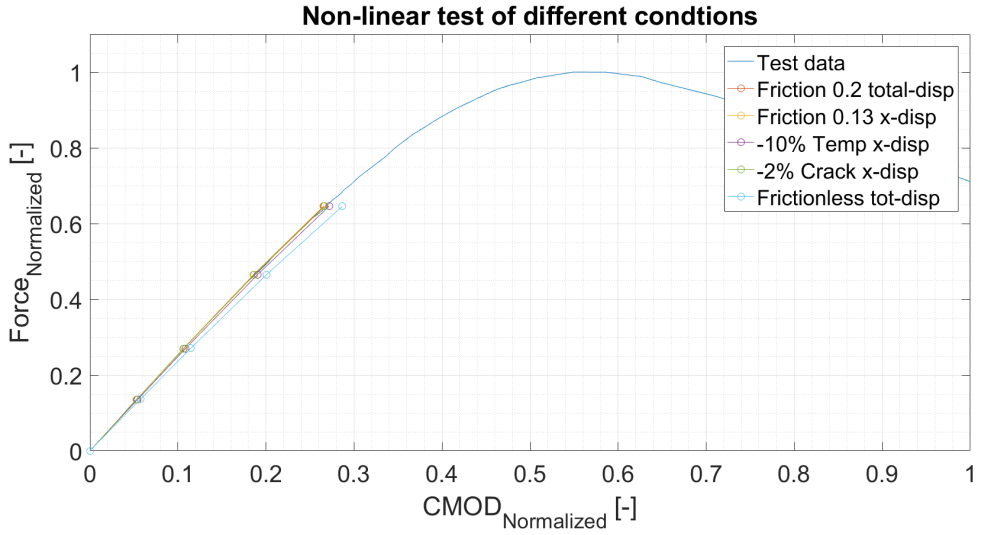

Figure 5.3: Prediction of force versus CMOD with linear material, under different conditions.

To further compare the influence of the different modifications, K_Q and K_{JQ} were calculated as described as in section 3. The results are presented in tables 5.1 and 5.2. The percentage difference calculated in stress intensity factor between simulation and tests, are rather small for all conditions. The only factor that is deemed to be a valid contender to friction in this comparison is measuring of the CMOD, in the x-direction instead of using the total displacement. The other modifications of properties seemed to be unrealistic. The test temperature is deemed to be well within 10%, and the crack size measurement is also deemed to be well within a 2% error margin for the total crack length. It was decided not to modify material properties as these were deemed to be correct.

Table 5.1: Comparison of different conditions with linear material K_Q.

Linear valid test	Diff K_Q test
Friction tot-disp	-3.59 %
Friction x-disp	-1.98 %
10% lower temp	-1.25 %
2% shorter crack	-5.12 %
Frictionless tot-disp	-1.25 %
K_Q test	0.00 %

Table 5.2: Comparison of different conditions with non-linear material for K_{JQ}.

Non-linear invalid test	Diff K_{JQ} test
Friction tot-disp	-1.31 %
Friction x-disp	0.29 %
10% lower temp	2.29 %
2% shorter crack	1.08 %
Frictionless tot-disp	3.67 %
K_Q test	0.00 %

5.2 Use of FE analyses to get further information from tests

5.2.1 Wallin ligament size dependency

Wallin [7] describes how general conclusions from historical data showed that the rising critical stress intensity had to do with the specimen width and not ligament size. However more recent understandings have shown that the ligament size is the crucial component. Wallin claims that this misunderstanding has to do with the focus on plane strain conditions. In order to be able to use smaller specimens Wallin suggest to use a ligament size dependent secant and remove the P_{max}/P_Q requirement. The size dependent secant would ensure a 0.5 mm crack growth at the critical load. To ensure a valid linear elastic stress intensity factor he propose a new excessive plasticity requirement of $1.5\frac{K_q}{\sigma_{ys}}^2$ or $1.1\frac{K_q}{\sigma_{ys}}^2$ if a 10% margin of error is acceptable. He also claims that the P_{max}/P_Q ratio requirement does not provide information about the critical stress intensity factor and penalizes materials with high resistance. However some materials will still need a rather large specimen size to meet even the $1.1\frac{\mathrm{K_Q}}{\sigma_{ys}}$ requirement.
Using example 7.1 in Anderson [1] a material that has a K_{IC} of 200 MPa $\sqrt{m}$ and a yield strength of 350 MPa would have to have a ligament size of $1.1\left(\frac{200}{350}\right)^2 = 0.35$ m = 350 mm

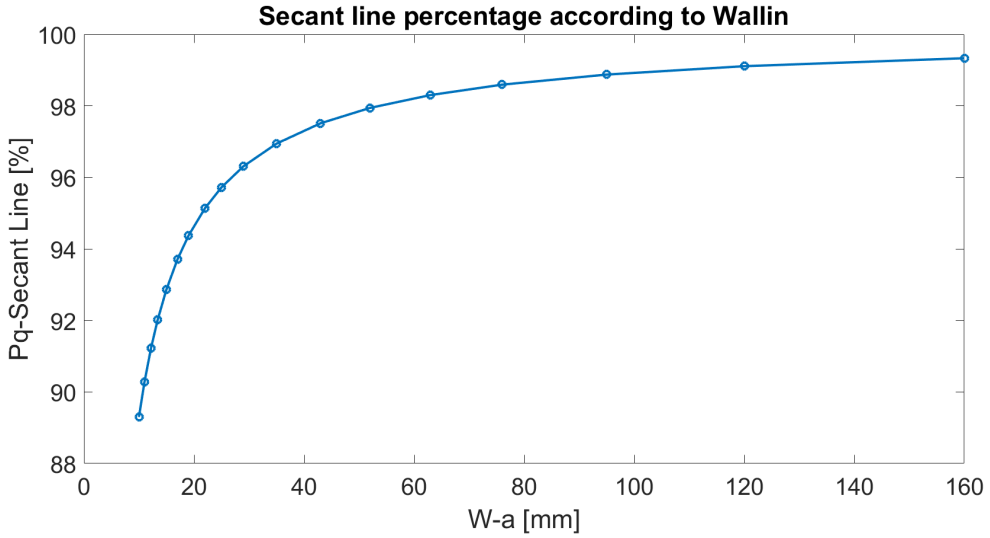

Figure 5.4: Secant using the Wallin approach.

5.2.2 Using FE analysis to retrieve a P_Q at 0.5 mm crack propagation

Barker [13] makes a case for non-linear elastic fracture analyses. He claims that if the specimen has a linear elastic unloading then the change in unloading compliance between two points of the force versus CMOD curve would be caused only by the increase in crack length, see figure 5.5. The ratio of plasticity during crack growth is defined as $p = \frac{\Delta x}{\Delta X}$.

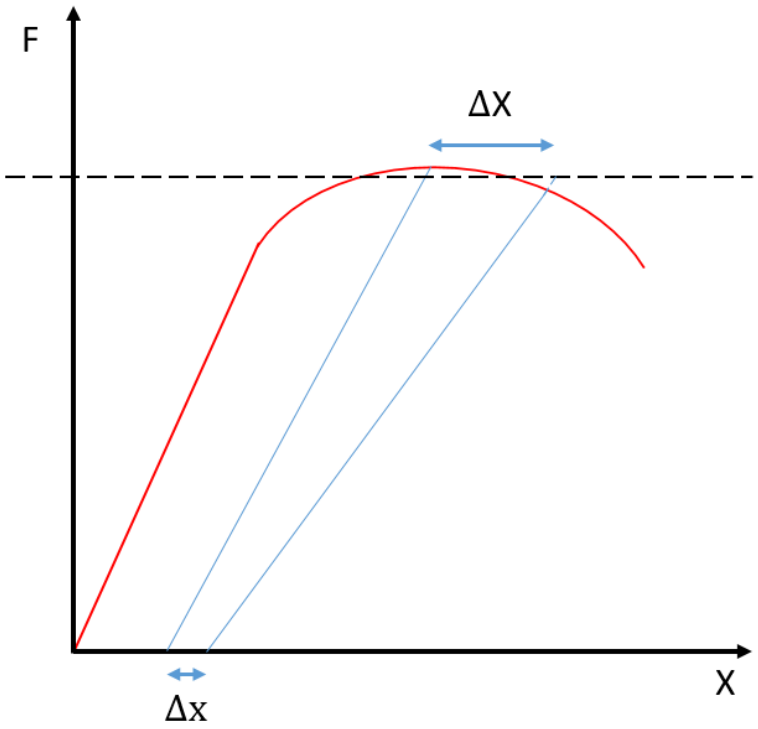

Figure 5.5: Force versus CMOD.

If the change of unloading compliance is fully linear elastic and only a consequence of crack extension, it would be possible to retrieve the same compliance numerically using FE analyses. If the change in plasticity when the crack is propagating is negligible then a P_Q should be able to be retrieved at 0.5 mm propagation using the non-linear response from FE simulations and the linear elastic FE response using an original and a 0.5 mm propagated crack. This is explained in figure 5.6 where ΔX is the difference in CMOD caused by crack growth.

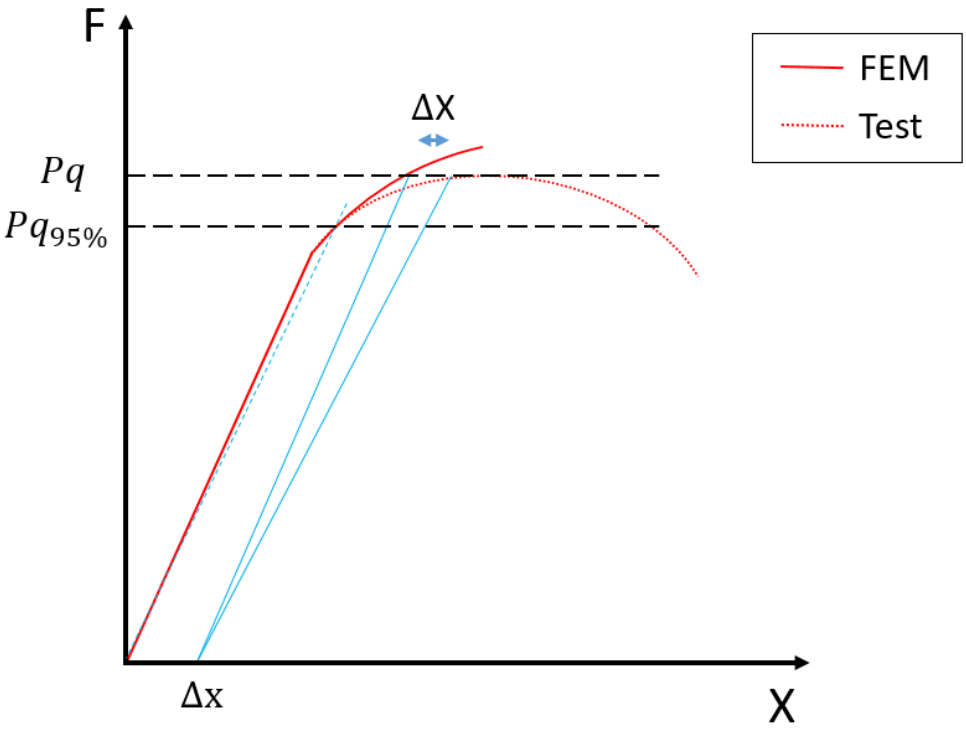

Figure 5.6: Non-LEFM P_Q determination.

This analysis was carried out for test 3 and resulted in a good force versus CMOD correlation between FE simulations and test data, it is found that the crack tip region clearly plasticized before crack growth. The result is shown in figure 5.7. The calibrations was made by matching the curve for the linear original crack with the curve for the non-linear original crack at the point where the linear propagated crack response matched the test data. See figure 5.8 for a close up. The result using this method shows that the crack has propagated 0.5mm at a much higher force than that described by the 95% secant.

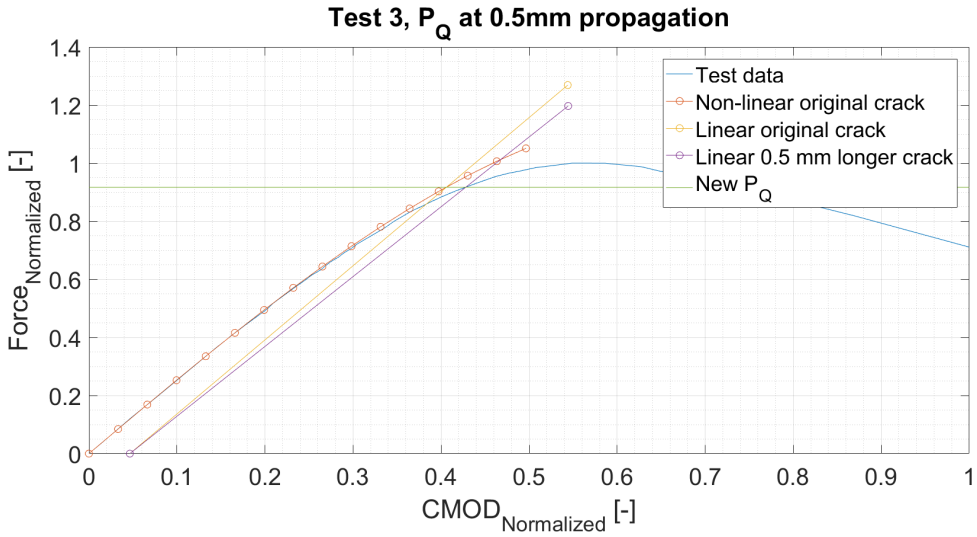

Figure 5.7: Non-LEFM Pq determination Real data

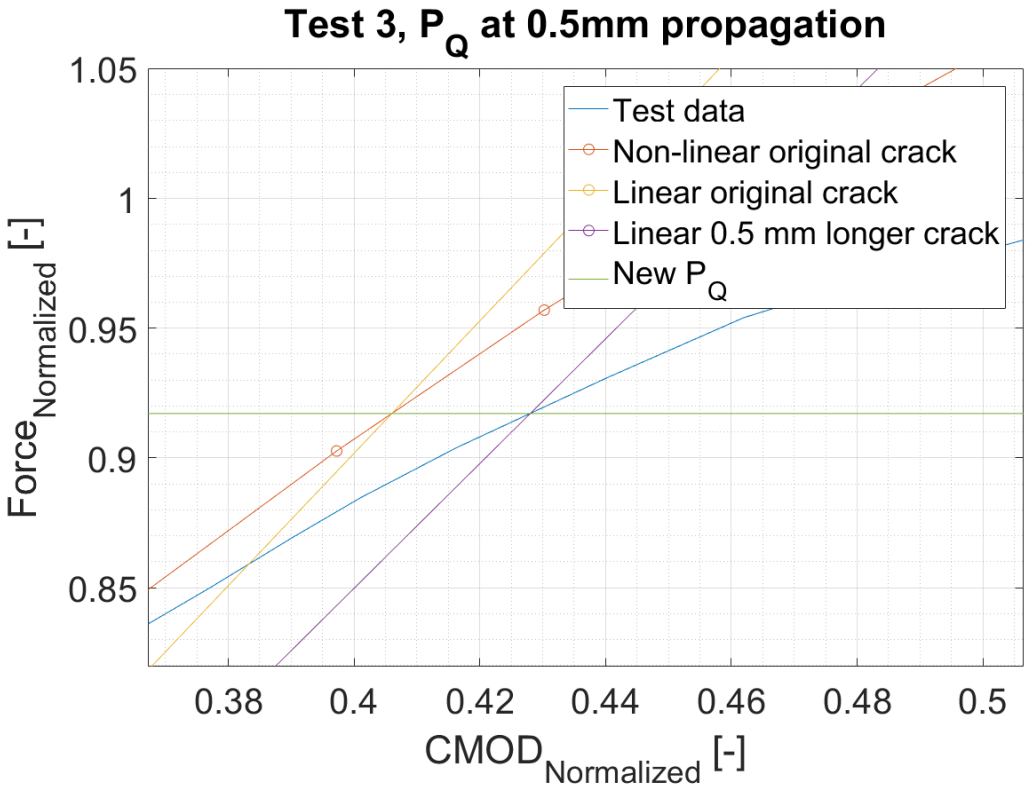

Figure 5.8: Close up of figure 5.7 at load levels close to P_Q

The stress intensity at the new candidate load P_Q thus also changed. Figure 5.9 shows the stress intensity K_{JQ} along the crack front, the mean K_{JQ} value along the crack front and the analytical value using eq 3.1 with the new P_Q and the geometry specified in the test report. The analytical evaluation seems to fit rather good to the K_{JQ} value along the crack front. However with this increase in K_Q, see table 5.3, the

plastic zone also increases and even with plastic zone of $1.1\frac{K_q}{\sigma_{ys}}$ Wallin recommended the ligament size would have to be twice the size to be valid. Further, this method was developed for a short rod specimen and not a CT specimen. Thus, this stress intensity value can not be classified as a K_{IC} value. Table 5.3 shows the difference in stress intensity K_{JQ}. Column 2 is the the difference in value between Ansys and the analytical value both at the new P_Q. Column 3 is the difference in value between Ansys at the new P_Q and the analytical at the old P_Q.

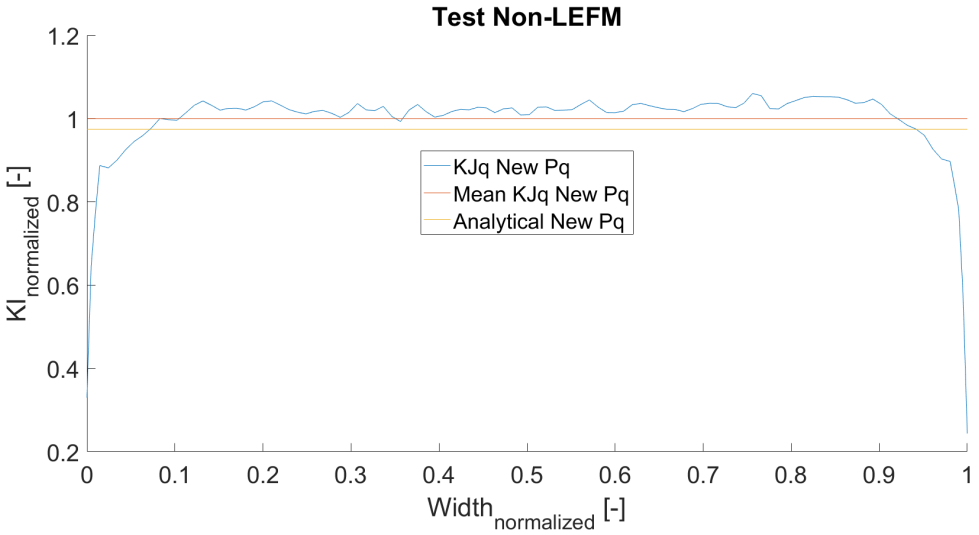

Figure 5.9: K_{JQ} result from non-linear and analytical evaluations

Table 5.3: Percentage difference between simulated solution and analytical stress intensity at new and old P_Q

.

Test	New K_Q	Old K_Q
Test 3	2.68 %	46.09%

5.3 Conclusions

- This thesis shows that it is possible to model and numerically recreate the fracture toughness test E399 using collected test data.
- The thesis adds to the conclusion that for a certain amount of plasticity, the 95% secant can not be used to derive K_{IC} as the crack has not propagated at that point.
- The thesis showed that for limited plasticity the J-integral can be used to calculate the linear elastic stress intensity factor.
- The thesis discussed the validity of adding friction to match the stiffness found in tested by comparing this to other ways of increasing the stiffness.
- The thesis discusses ways of using FE analyses to derive information from invalid tests.

5.4 Future work

Recommendations for future work based on this thesis is presented in this section.

- Cohesive zone crack propagation. To further describe the force CMOD curve crack propagation should be examined.
- Validity of using friction. Tests using different materials with different geometries could be tested to see if the friction coefficient is needed for those as well.
- Make a study using the method described in section 5.2.2 by using different geometries for the same material which fall between $2.5(K_Q/\sigma_{ys})^2$ and $1.1(K_Q/\sigma_{ys})^2$ to see whether this method can be used to get a consistent K_{IC} values. To get the K_{IC} for the tests studied in this thesis bigger specimens are needed or, alternatively to use the test method E1820.

References

[1] Anderson, T L. (2005). *Fracture Mechanics - Fundamentals and Applications 3rd Ed* Taylor Francis Group, LLC

[2] Ekberg A and Andersson H, (2019). *Non-linear fracture mechanics - a brief overview Ed 2.3*, Gothenburg, Chalmers

[3] E.Dowling N, (2013). *Mechanical Behavior of Materials - Engineering Methods for Deformation, Fracture and Fatigue 4th Ed*, Essex, Pearson Education Limited

[4] *ASTM E399, Standard test method for linear-elastic plane strain fracture toughness KIC of metallic materials.* American Society for Testing and Materials; 2011.

[5] *ASTM E1820, Standard terminology relating to fatigue and fracture testing.* American Society for Testing and Materials; 2011.

[6] Xian-Kui Z and James J A., 2012. *Review of fracture toughness (G, K, J, CTOD, CTOA) testing and standardization* Elsevier.

[7] Kim R. W. Wallin (2005). *Critical Assessment of the Standard ASTM E 399* Journal of ASTM International, April 2005, Vol. 2, No. 4

[8] R. T. Bubsey, M H. Jones and W F. Brown Jr (1969) *Clevis Design For Compact Tension Specimens Used In Plane-Strain Fracture Toughness Testing* Washington DC, National Aeronautics and Space Administration.

[9] Pook. L.P. (1968) *The Effect Of Friction On Pin Jointed Single Edge Notch Fracture Toughness Test Specimen* (The International Journal Of Fracture Mechanics, Vol. 4, Nr. 3) Groningen, Wolters-Noordhoff Publishing.

[10] Behzad V. Farahania,b, Paulo J. Tavaresa, Jorge Belinhaa, P. M. G. P. Moreiraa 2019 *A Fracture Mechanics Study of a Compact Tension Specimen: Digital Image Correlation, Finite Element and Meshless Methods* (2nd International Conference on Structural Integrity, ICSI 2017, 4), Porto, Portugal, INEGI, Institute of Science and Innovation in Mechanical and Industrial Engineering and FEUP, Faculty of Engineering, University of Porto.

[11] Y. Mohammed, Mohamed K. Hassan, A. M. Hashem (2012) *Finite Element Computational Approach of Fracture Toughness in Composite Compact- Tension Specimen* (International Journal of Mechanical Mechatronics Engineering IJMME-IJENS Vol:12 No:04.) South Valley University, Qena, Egypt

[12] A. A. Nassar, E. G. Fayyad, (2019) *Linear and Non-Linear Stress Analysis for the Prediction of Fracture Toughness for Brittle and Ductile Material using ASTM E399 and ASTM E1290 By ANSYS Program package* (IOP Conf. Series: Materials Science and Engineering579 (2019)) Basra university /Mechanical En-

gineering Department/Basra/Iraq, Basra Oil Company / South Rumelia/design project Department/ Basra/Iraq

[13] L M. Barker (1978). *Theory for determining K_{IC} from small non-LEFM specimens, supported by experiments on aluminum* (International Journal of Fracture, December 1979, Vol. 15, No. 6), Salt Lake City, Utah, USA, TerraTek